PERGAMON

Progress in Surface Science 71 (2003) 185–215

Progress in SURFACE SCIENCE

www.elsevier.com/locate/progsurf

Review

Atomic structure of InAs quantum dots on GaAs

K. Jacobi *

Fritz-Haber-Institut der Max-Planck-Gesellschaft, Faradayweg 4-6, D-14195 Berlin (Dahlem), Germany

Abstract

In recent years, the self-assembled growth of semiconductor nanostructures, that show quantum size effects, has been of considerable interest. Laser devices operating with self-assembled InAs quantum dots (QDs) embedded in GaAs have been demonstrated. Here, we report on the InAs/GaAs system and raise the question of how the shape of the QDs changes with the orientation of the GaAs substrate. The growth of the InAs QDs is understood in terms of the Stranski–Krastanow growth mode. For modeling the growth process, the shape and atomic structure of the QDs have to be known. This is a difficult task for such embedded entities.

In our approach, InAs is grown by molecular beam epitaxy on GaAs until self-assembled QDs are formed. At this point the growth is interrupted and atomically resolved scanning tunneling microscopy (STM) images are acquired. We used preparation parameters known from the numerous publications on InAs/GaAs. In order to learn more about the self-assemblage process we studied QD formation on different GaAs(0 0 1), (1 1 3)A, and $(\bar{1}\,\bar{1}\,\bar{3})$B substrates. From the atomically resolved STM images we could determine the shape of the QDs. The quantum "dots" are generally rather flat entities better characterized as "lenses". In order to achieve this flatness, the QDs are terminated by high-index bounding facets on low-index substrates and vice versa. Our results will be summarized in comparison with the existing literature.

Keywords: Molecular beam epitaxy; Scanning tunneling microscopy; Growth; Surface structure, morphology, roughness, and topography; Quantum dots; Gallium arsenide; Indium arsenide; Single crystal surfaces

* Tel.: +49-30-8413-5201; fax: +49-30-8413-3155/5106.
E-mail address: jacobi@fhi-berlin.mpg.de (K. Jacobi).

0079-6816/03/$ - see front matter
doi:10.1016/S0079-6816(03)00007-8

Contents

1. Introduction

Self-assembled quantum dots (QDs) have been extensively studied in recent years because of their potential for technological applications [1–3]. QDs are small three-dimensional ensembles of a low-band-gap semiconductor as InAs embedded in a wide-band-gap semiconductor matrix as GaAs. Such semiconductor nanostructures exhibit quantum size effects for the localized electrons or holes: The InAs ensemble produces a confinement potential for electrons in the conduction band and for holes in the valence band. The separation between the corresponding energy levels should be larger than about 0.2 eV so that the higher lying levels are unlikely to be populated by thermal activation at room temperature. This sets an upper limit for the dot diameter of about 20 nm equivalent to about a line of 80 atoms for the diameter and about 60,000 atoms for the overall size. A lower limit is given by the condition that at least one bound level should exist which means a minimum of about 5 nm or 20 atoms in diameter and 1000 atoms in overall size. In order to achieve good intensity in electro-optical devices a number density for such QDs of about 10^{10} cm^{-2} should be reached. Furthermore, the size distribution should be rather narrow in order to produce appropriate line widths in, e.g., QD laser applications. Interestingly, laser devices operating with self-assembled InAs QDs embedded in GaAs have already been demonstrated [1–3]. This development was initiated in 1990 when it was shown that dislocation-free strained InAs islands self-assemble when InAs is grown on a GaAs(001) substrate [4].

A rather plausible explanation of self-assemblage is derived in a thermal-equilibrium picture taking advantage of the Stranski–Krastanow (SK) growth mode [5] which often applies for heteroepitaxy in systems with lattice mismatch $\geqslant 2\%$ such as InAs/GaAs (7.2%). Theoretical work has addressed the formation phenomena of QDs and attempted to predict their size and number density. So far, the accuracy of calculations addressing the SK growth mode [6–16] is limited in part by the lacking knowledge of the QD shape. While most theoretical calculations, particular those which are based on thermodynamical descriptions, have assumed that only surfaces with low Miller indices occur as bounding facets of the QDs, from experiments the occurrence of facets with high Miller indices was concluded [17–22]. (For a better orientation we include the stereographic triangle as Fig. 1 where we have marked all high-index surfaces mentioned in this contribution.) Thus, the determination of the exact shape of the QDs is needed to substantiate the theoretical models and thereby to support the device technology.

The experimental determination of the QD shape is a difficult task. So far, experimental work has focused on varying the growth conditions to control the size and improve the uniformity of the QDs [1–3]. In our work we have focused on the shape of the QDs but exclusively for the InAs/GaAs system. Our way of approaching

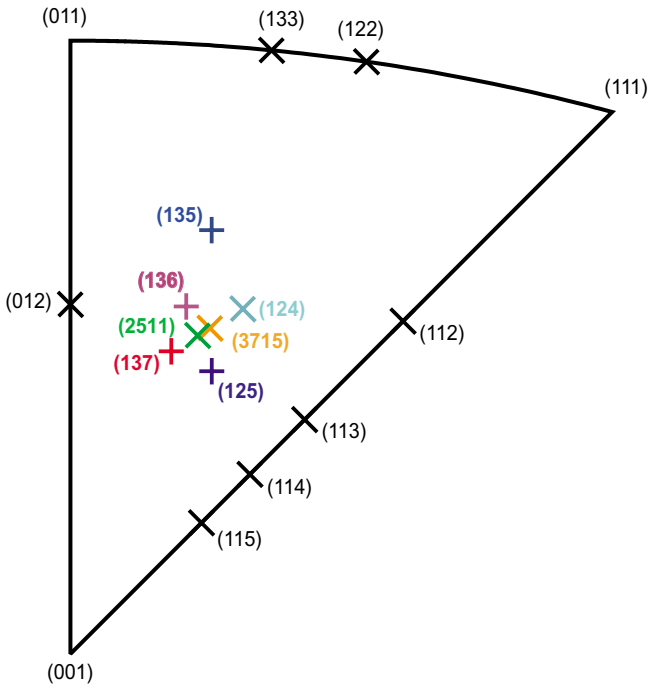

Fig. 1. Stereographic triangle for fcc III–V compound semiconductor surfaces exhibiting the low-index corner points, the [$\bar{1}$ 1 0]-zone borderline connecting the (0 0 1) and (1 1 1) corner points, and the different high-index surface orientations touched upon in this contribution.

this problem is to interrupt the preparation process after formation of the QDs and to look at them in situ by scanning tunneling microscopy (STM). Although the QD shape may alter during following overgrowth—in order to embed the QDs for device applications—our approach delivers the structure of QDs evolving in the first step of self-assemblage.

Most studies on InAs QDs have been performed on GaAs(0 0 1) substrates to some of them reference has been given already in the context of resolving facets [17–22]; some other representative examples [23–28] will be also discussed below. InAs QDs have been observed not only on GaAs(0 0 1) but also on GaAs(1 1 3)A [29,30] and GaAs($\bar{1}\,\bar{1}\,\bar{3}$)B [29–32]. From reflection high-energy electron diffraction (RHEED) observation of the SK growth mode (see below) and photoluminescence, Fortina et al. [32] concluded on QDs for GaAs(1 1 N)A and B with $N = 2$–5. On the other hand, InAs grows with introduction of dislocations in the 2D layer-by-layer growth mode on GaAs(1 1 0) [30,31], GaAs(1 1 1)A [31,33,34], and GaAs($\bar{1}\,\bar{1}\,\bar{1}$)B [35]. On the one hand, the substrate orientation is responsible for the appearance of specific bonding facets on the islands that determine their shape, which in turn defines the electronic structure. On the other hand, the substrate reconstruction influences the kinetic processes of adsorption, migration, and incorporation of atoms in heteroepitaxy as well as can directly influence the mechanism and velocity of strain relief producing a change in the island sizes and distributions. It is therefore interesting to compare the formation and development of the InAs QDs grown on the GaAs(0 0 1), GaAs(1 1 3)A [36,37], and GaAs($\bar{1}\,\bar{1}\,\bar{3}$)B surfaces [38–40], the latter two having the same crystallographic orientation but different atomic terminations.

The reconstruction and orientation of the substrate certainly plays a crucial role in the heteroepitaxial growth of highly mismatched materials. With the change of the substrate we also expect a change of the symmetry of the QDs if the growth is epitaxial. It has been shown experimentally that on the high-symmetry GaAs(0 0 1) surface the shape of InAs QDs exhibits the same two mirror-symmetry planes as the bulk-truncated (0 0 1) substrate. Four bounding facets, derived from STM [22] or RHEED [20] observations, frame nearly the whole body of the QD and grow with equal rates because of the same reconstruction and the same elastic energy density on each facet. By using high-index substrates the symmetry is lowered, e.g., GaAs{1 1 3} surfaces exhibit only one symmetry plane normal to the bulk-truncated surface. Therefore, only two facets are expected with equivalent growth rate and, because the 3-D islands cannot be framed with two facets alone, other surfaces with different growth rate are expected to develop. Thus, the preferential migration of In atoms among the different bounding facets from the slower to the faster growing facets, the so-called inter-surface diffusion, should be taken into account. Therefore, we expect that the interplay of different growth rates of the facets may determine the shape of the QDs on the high-index substrates.

In this report we summarize the results on the shape of InAs QDs on GaAs(0 0 1), GaAs($\bar{1}\,\bar{1}\,\bar{3}$)B, and GaAs(1 1 3)A surfaces. Most surprisingly, the shape of QDs on the GaAs(0 0 1) substrate is given to a large part by {1 3 7} facets [22], a high-index surface unknown till recently. The GaAs(1 1 3)A [36,37] and GaAs($\bar{1}\,\bar{1}\,\bar{3}$)B [38–40] surfaces are also appropriate substrates as their stability has been demonstrated

earlier. First, we could demonstrate that the bounding facets appearing on the QDs are inclined with the same angles to the substrate in both cases, but that the overall shape of the QDs is different. Also, each QD is developed with the same orientation relative to the substrate, with mirror symmetry to the $(\bar{1}\,1\,0)$ plane perpendicular to the surface, and exposes $\{1\,1\,0\}$ and $\{1\,1\,1\}$ surfaces as bounding facets. Second, the unequal atomic arrangement on both bare GaAs surfaces and on the subsequently grown InAs wetting layers, determines different morphological response to the misfit strain and results in different size and size distribution of the QDs. So, the QDs on GaAs$(\bar{1}\,\bar{1}\,\bar{3})$B sit on a flat base terminated by high-index surfaces whereas the QDs on GaAs(1 1 3)A do not.

2. Stranski–Krastanow growth mode

Before we review the atomic shape of the QDs on different GaAs substrates, we make some general remarks on the QD formation process which is sketched schematically in Fig. 2. The aim of this chapter is not to give a complete review, but to

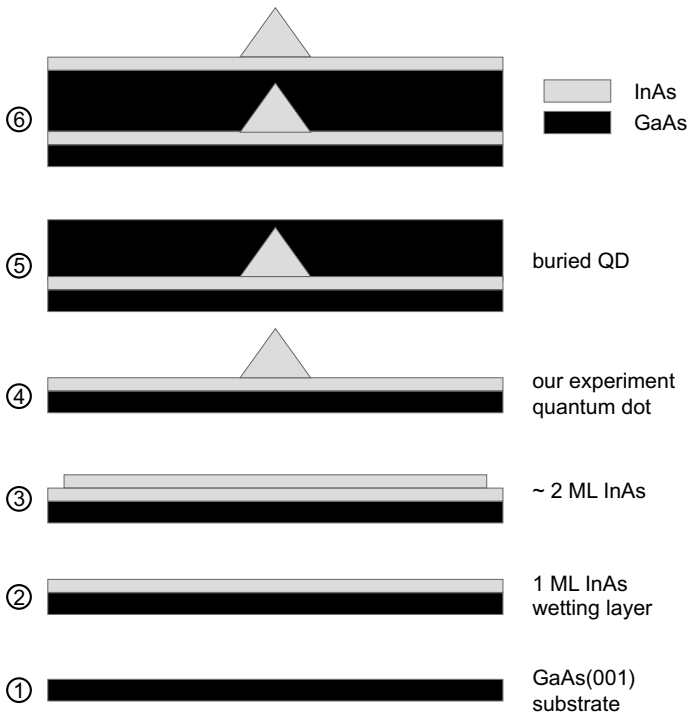

Fig. 2. Schematic growth sequence with six steps for the preparation of a QD system. At the 4th step our STM experiments were performed after self-assemblage of the QDs in the first QD layer on top of the wetting layer.

more explicitly introduce the arguments of why it is necessary to evaluate the individual shapes of QDs in order to understand the QD formation in an atomistic view.

Generally, the self-assemblage of QDs is understood to occur during SK growth mode in heteroepitaxy: At a critical thickness of the epitaxial InAs layer (step 3 in Fig. 2) 3-D islands or QDs form on top of a wetting layer which is largely composed of the deposited material. This process is called islanding or SK transition. These islands can be completely embedded then by additional overgrowth—with material of the same kind as the substrate—establishing an ensemble QDs. In the SK growth mode, islands form when the strained heteroepitaxial film reaches a given thickness because the material can better relax in slightly strained islands than in a heavily strained film. Thereby the gain in elastic energy compensates for the energy cost due to the increase in surface area. The residual strain in the islands can be further reduced by incorporation of dislocations at the interface.

From a number of different experimental techniques as transmission electron microscopy (TEM), cross-sectional STM (X-STM), and optical methods as luminescence from excitonic excitation, the following picture has emerged [1–3]: For a system as InAs in GaAs, QDs are formed having a size of about several 10^4 atoms at a number density of 10^9–10^{11} QDs cm^{-2}. The sharpness of the luminescence light indicates that the size distribution is quite narrow. These observations have to be explained in theory.

Unfortunately, there is no theory available till now, to completely describe the QD formation. Even the question is being discussed whether the dot formation is governed by kinetics or energetics. For a detailed review of the existing theories the reader is referred to the contributions of Wang et al. [15,16]. Among the different models there is no question about that strain relief is the main driving force for the transition from the strained-layer to the dot-on-layer system. It seems to be very reasonable that the gain from strain relief, which is proportional to the volume V of the QD, is in balance with the increase of surface area, which is proportional to $V^{2/3}$. One may speculate that also the creation of edges is contributing but it turned out that this effect is only marginal [14–16]. Such a model was applied to the InAs on GaAs system and it was found that a truncated pyramid with (1 1 0) as well as (smaller) (1 1 1) side facets evolves as equilibrium shape of the QD [14]. We note here that there is an underlying assumption used in this theory that only low-index surfaces as (1 0 0), (1 1 0), and (1 1 1) are of low-energy, i.e., appropriate to terminate a QD. In the mean time we have discovered that there is another low-energy surface within the stereographic triangle which is (2 5 11) [41–43] and contains two (1 3 7) unit cell in its own unit cell making (1 3 7) a further candidate for terminating the QD.

An equilibrium theory with only two energetic contributions fails to predict a finite equilibrium size of the QDs which gives rise to the sharp size distribution found in experiment. The dots tend to become larger on the expense of their number density. Recently, Wang et al. [15] could overcome this problem by assuming that the system is "trapped in a constrained equilibrium state, where the size is determined by the island density and the nominal coverage". The constraint is that the island

density is kept fixed during growth. These authors also took into account the surface energy of the wetting layer which turned out to increase with the overall volume to be distributed and to act as a third term in the energy balance providing this way an optimal size of the QD. It should be mentioned that also in this theory a low-energy, high-index surface was not considered.

These short remarks clearly indicate that experiments in order to evaluate the actual shape of the QDs are highly demanding. Also, it seems to us that Monte-Carlo simulations using ab initio energy barriers for the atomic processes during growth would be very useful in modeling QD formation but are still beyond the capabilities of our nowadays computer capabilities. Recently, e.g., such a simulation was performed for the homoepitaxial growth of a fraction of a monolayer of atoms and their transition to 2D clusters on a grid of 250×250 sites [44]. For our purpose one would have to model a system of heteroepitaxy of a compound semiconductor and of many 3-D dots of a size of several 10^4 atoms.

3. Experimental determination of the quantum-dot shape

To determine the QD shape is a very difficult task. This is a principal obstacle for all kinds of buried interfaces. A powerful method certainly is TEM which has been applied to the InAs/GaAs system rather early [17,23,45–47]. In plain-view TEM the main problem is the modeling of the contrast. Besides the chemical contrast of In versus As in case of InAs there is also the contrast due to strain between InAs and GaAs. These two effects have to be disentangled, i.e., modeling has to be performed in order to interpret the observed images. Quadratic pyramids with {1 1 0} side facets have been inferred from plain-view TEM images rather early [45,46]. However, inspection of these images raises some doubt on the conclusiveness of these results. This is in accord with a more recent statement of Liao et al. [47] "that the on-zone bright-field image contrast of QDs will reflect the symmetry of the lattice rather than the symmetry of the QD".

Another powerful method is X-STM where X stands for cross-sectional. For this approach samples with QDs embedded in a semiconductor matrix were cleaved along a (1 1 0) cleavage plane and then studied by STM. If one is lucky, the cleave is through one or several QDs and one may find them in the approach of the STM tip. The InAs/GaAs system has been studied from several groups [48–50]. Dähne and coworkers [50] could successfully analyze STM images of this kind for QDs grown by metal-organic vapor phase epitaxy (MOVPE). (MOVPE is mentioned here because otherwise we concentrate on systems prepared through MBE.) But again, the observed images have to be analyzed with some care as at least the uppermost surface layer in the cleavage plane of the QD relaxes outwards (perpendicular to the cleavage plane) and one has to take into account electronic and topographical effects in analyzing the STM images. The first striking result is that the QDs are not high pyramids but are strongly truncated. So, the dots are flat entities better described as lenses as some authors used to do. Since the QDs are only about five atomic layers high, it is also not very straightforward to analyze the side facets. Furthermore, one

has to keep in mind that one individual QD exposes in X-STM only one given cleavage plane and any conclusion on a general shape of the QDs must be derived from averaging over many QDs. This is quite different for our in situ STM images of unburied QDs as described later in this contribution in which a single QD can be depicted with all of its facets.

Finally, structure information can also be acquired in situ during QD growth in MBE by RHEED. Generally, RHEED is used during MBE growth and very clearly indicates the transition in the growth mode from layer-by-layer to SK as the RHEED pattern changes from streaky—indicative of layer growth to spotty—indicative for 3-D islanding. Interestingly, with the electron beam of RHEED along $[1\,\bar{1}\,0]$, the spots acquire a V-shaped form called chevron. (see Fig. 11 below). This indicates that the QDs are terminated by facets inclined by only a small angle with respect to the substrate plane so that the beam, diffracted from these facets, falls onto the screen. Many other groups working in the field have made this observation [17,20]. Lee et al. [20] have analyzed the direction of the chevron and concluded that the facets are of (1 3 6) orientation. We believe that within the experimental accuracy this is identical to our (1 3 7) orientation [22] discussed below. We will also show that we could unambiguously assign the exact facet orientation by determining the atomic structure of the facets.

In our experiment we prepared InAs layers on a number of different GaAs substrates. The SK transition was observed by the RHEED pattern, which turned from streaky to spotty. At this moment the heating was shut off and the Knudsen cells were closed. As our sample carrier is rather bulky (a 55 g heavy Ta block) the temperature drop is rather slow: From 600 to 500 °C in 1 min and from 600 to 400 °C in 2.5 min. On the other hand the stop of In flux terminates growth without destroying the developed QD structure, as there is enough As_2 pressure in the background, which is pumped off by the cryopanels not so quickly. So, we conclude that the growth is stopped but that the achieved structures have some time to reach a stable situation under As-rich conditions.

Our experiments were carried out in a multi-chamber ultrahigh-vacuum system, which was equipped with a small molecular-beam epitaxy (MBE) chamber and an STM chamber (Park Scientific Instruments, VP2) as described in detail elsewhere [51]. Samples with a typical size of about 5×10 mm^2 were cut from a GaAs wafer (mostly n-type, Si-doped, carrier concentration 1.4–4.8×10^{18} cm^{-3}, Wafer Technology). The samples were cleaned by several ion bombardment and annealing cycles. Afterwards GaAs buffer layers about 50 nm thick were deposited using MBE at 530 °C. The temperature was measured by a pyrometer that was calibrated against the GaAs(0 0 1) c(4×4) to $\beta 2(2 \times 4)$ transition at 465 °C. Then the samples were cooled down to a growth temperature between 435 and 470 °C and InAs was deposited. The growth rate of InAs was about 0.005 nm/s. The beam equivalent pressure ratio of As_2 /In was 40–50 at an As_2 pressure of $\sim 7 \times 10^{-7}$ mbar. The nominal amount of InAs deposited onto the surface was 1.4–2.9 monolayer (ML). The sample heater and the In- and As-Knudsen cells were shut off immediately, as soon as the RHEED pattern changed from streaky to spotty. Then the samples were transferred to the STM chamber within less than one minute without breaking the

vacuum. STM images were acquired from the uncapped QDs at room temperature in constant current mode.

4. InAs quantum dots on GaAs(0 0 1)

The InAs/GaAs(0 0 1) system is very important because most applications rely on it. Already in 1990 it has been observed that dislocation-free, strained islands form by itself when $In_{0.5}Ga_{0.5}As$ is deposited on GaAs(0 0 1) [4]. (As, at least at the interfaces between InAs and GaAs, there is intermixing between Ga and In, we include $In_xGa_{1-x}As$ in our considerations.)

Nabetani et al. [17] performed RHEED and plain-view TEM experiments. From the chevron reflexes in RHEED they concluded on two {1 1 3}A facets on the QDs. The shape of the QDs was found to be laterally asymmetric: 15.0 ± 3 nm along $[1\,\bar{1}\,0]$ and 13.3 ± 2 nm along [1 1 0]. We believe that these findings are in good accord with our own results [22].

Moison et al. [18] performed RHEED and ex situ atomic force microscope (AFM) measurements on MBE grown InAs QDs on GaAs(0 0 1). They observed a critical thickness of 1.75 ML from which on QDs are formed. At about 3 ML coalescence occurs. First QDs formed were 3 nm high and 24 nm in diameter at the base giving rise to an aspect ratio(AR) of 0.13. These values increase to, e.g., 4 and 30 nm at 2.35 ML ($AR = 0.13$). The authors claimed to observe facets, with facet planes ranging from (4 1 0) for the small dots and (1 1 0) for the largest ones. At about 3 ML, when coalescence starts to occur, the lateral sizes reached the interdot mean distance indicating that no exchange of matter between dots is possible before they touch each other. The authors pointed out that all QDs with the same volume have the same shape whatever the coverage, at which they are obtained, showing that individual dots take their equilibrium shape. They considered the question of the existence of dislocations in the QDs to be open although strong photoluminescence seemed to rule it out. Interestingly, the thickness of the wetting layer was found to decrease with InAs coverage and to vanish around coalescence, a behavior that departs from the classical SK growth model.

Using atomic force microscopy (AFM), Leonard et al. [23] observed self-assembled InAs QDs during MBE growth on GaAs(0 0 1) above a critical thickness of 1.5 ML. The mean diameter of the QDs decreased from nearly 30 to 20 nm at higher (1.9 ML) coverage. The height was 6–8 nm giving rise to aspect ratios between 0.2 and 0.4. With increasing InAs coverage, the size of the QDs did not increase—it even slightly decreased—instead the nucleation density increased. At a number density of approximately 4×10^{10} cm^{-2}, large relaxed islands formed and the density of QDs did not increase. The authors could not atomically resolve the shape of the QDs but concluded the shape to be ''radially symmetric and planoconvex, similar to a lense'' [23].

Ikoma and Ohkouchi [24] used in situ STM on GaAs(0 0 1) substrates misoriented by 1° towards [1 1 0]. The critical thickness was 1.8 ML. Most of the QDs had a size of about 15 nm in $[1\,\bar{1}\,0]$ direction, 10 nm in [1 1 0] direction, and about 2 nm in

height (AR = 0.16). The lateral anisotropy is in agreement with our results. They could not resolve the atomic structure of the facets of the QDs. At 2.0 ML of InAs the number density was 3×10^{11} cm^{-2}. From resolving the atomic structure of the wetting layer being typical for InAs, they concluded that the QDs grow on top of the wetting layer. Finally, about 85% of the QDs were formed near the step edges on the lower terraces.

Hasegawa et al. [19] performed in situ STM investigation on MBE prepared InAs QDs on GaAs(0 0 1) very similar to our own experiments. They observed coherent QDs between 1.6 and 3.0 ML. At 1.6 ML the QDs were 4 nm high and 17 nm at the base along [1 1 0] and 23 nm along [$\bar{1}$ 1 0] giving an aspect ratio of 0.2. Whereas the lateral dimensions kept nearly the same up to 3 ML, the height increased to 7 nm. They concluded that the side facets changed from (1 1 4) to (1 1 3). For some QDs they also observed a different facet which they assigned to (2 1 5). This orientation is near to our (1 3 7) facet and we will come back to this point below. From 3 ML on they observed larger, apparently incoherent islands.

Lee et al. [20] studied MBE grown InAs QDs on GaAs(0 0 1) and concluded from the V-shaped RHEED reflexes on four {1 3 6} oriented facets to define the QD shape. This observation and also conclusion is very similar to our own result [22] to be discussed below. Using AFM the same authors studied the critical layer thickness with temperature [27]. They concluded that surface adatom diffusion and In desorption are the controlling processes. Under conditions in which In desorption is significant, the islanding transition is reversible. During the reverse process the size distribution becomes bimodal. The larger islands form at step edges eventually due to reduced strain in this area. We think that the latter may also be due to incorporation of dislocations.

Joyce et al. [21] extensively studied InAs QDs on (0 0 1), (1 1 0), and (1 1 1)A oriented substrates of GaAs. For (0 0 1) they got some atomic resolution with in situ STM. The QDs are oriented quite similar to ours; from the facet angle with respect to the substrate they concluded on {1 1 3}/{1 1 4} for the facets showing to [1 1 0] and [$\bar{1}\,\bar{1}$ 0] and on {1 1 5} ones for those showing to [$\bar{1}$ 1 0]. The facet assignment differs from ours [22].

Solomon et al. [25] used TEM and nicely showed that InAs QDs can be stacked up to 10 layers. They also demonstrated that the QDs are coherent. They did not draw any conclusion on the QD shape.

Heitz et al. [26] studied the formation of InAs QDs by in situ STM. They found the critical thickness at about 1.6 ML. Below this value they observed a variety of 2D and 3-D clusters occurring and going away again. They did not resolve the atomic shape of the QDs. No details of QD size were given.

Saito et al. [28] used ex situ AFM and studied the dependence of the QD size from growth temperature between 440 and 570 °C. The size increases with temperature and the number density decreases indicating control of the growth, at least partly by kinetics. For a growth controlled by energetics one expects the size to decrease with increasing substrate temperature. The aspect ratio changes at a given volume from 0.20 to 0.33. This is rationalized in a simple model according to Ross et al. [52].

It is interesting to note that all these observations are in very good agreement with our results [22]. The only deviation consists in the claimed quadratic pyramids with the steep {1 1 0} side facets [45,46]. We have this critically discussed already above. The preparation parameters used in our case are very similar to the values used in other studies. Therefore, we believe that our results are very likely applicable to all systems in the above mentioned contributions.

We now turn to our own measurements on InAs QDs on GaAs(0 0 1), the main results being published already elsewhere [22,53]. Here we give a summary and include some additional information which set these data in a better perspective. Fig. 3(a) gives an overview STM on a 500×500 nm^2 scale. From visual inspection of Fig. 3(a) as well as from the diagram in Fig. 3(b) one recognizes that the size distribution of the QDs is relatively sharp. Fig. 3(a) contains 489 QDs which is equivalent to a number density of 1.9×10^{11} QDs cm^{-2}. About half of the QDs have a diameter of 12.5 ± 1.0 nm and the mean height is 2.2 nm resulting in an aspect ratio of AR $= 0.18$. These values are in good accordance with values from the literature [17–28].

Large-area changes in brightness in the background of Fig. 3 are due to the structure of the wetting layer and especially due to mono-atomic steps. The steps are better recognized in Fig. 4 that reproduces a STM image in differentiated form which emphasizes the step edges. The gray scale is adjusted so that the InAs wetting layer is clearly recognized. It is interesting to note that the QDs tend to attach near a step edge at the lower terrace. This is in agreement with results of Ikoma and Ohkouchi [24]. Small islands (see arrow in Fig. 4) are preferentially observed in the middle of a

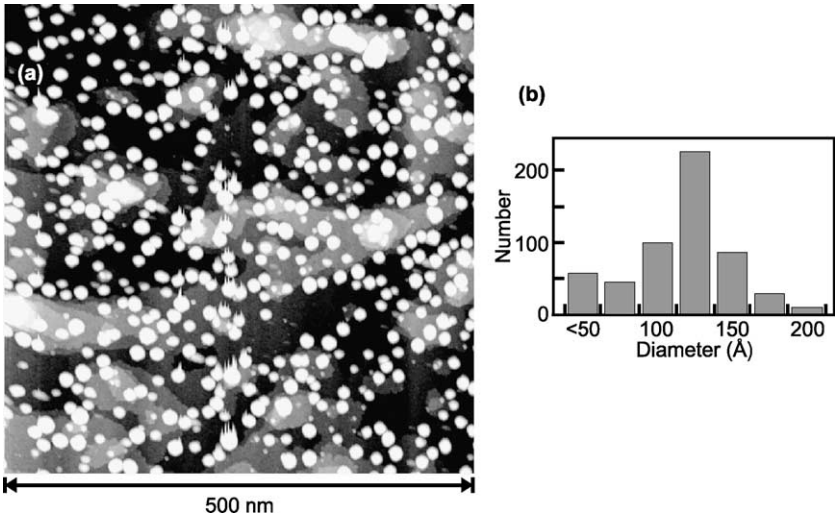

Fig. 3. (a) STM image of InAs QDs on GaAs(0 0 1). InAs was deposited at 450 °C at a rate of 0.05 Å s^{-1} (sample bias voltage $U = -2.25$ V; sample current $I = 0.19$ nA). The number density of the QDs is 1.9×10^{11} cm^{-2}. (b) Histogram of QD size from the STM image in (a). From [53].

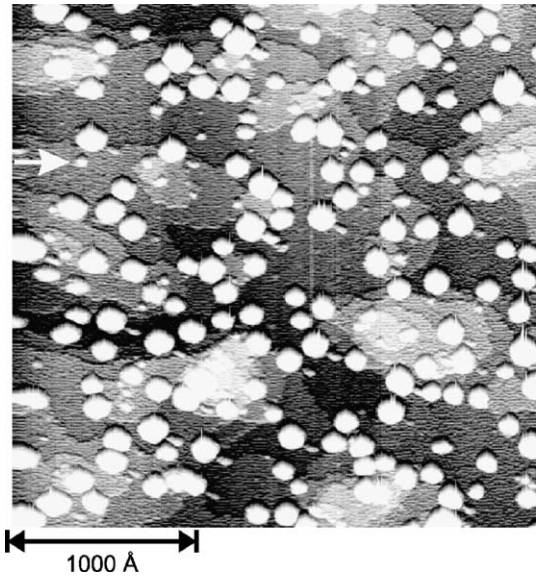

Fig. 4. Derivation of an STM image of InAs QDs on GaAs(0 0 1) (sample bias voltage $U = -2.75$ V; sample current $I = 0.15$ nA). The arrow indicates a small island in the middle of a terrace. From [53].

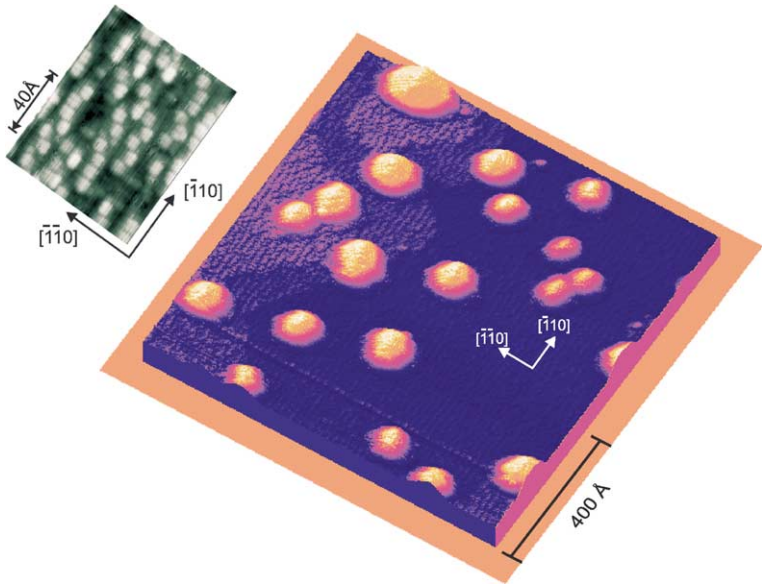

Fig. 5. 3-D STM image of InAs QDs on GaAs(0 0 1) (sample bias voltage $U = -2.75$ V; sample current $I = 0.15$ nA). The wetting layer is atomically resolved and depicted in the adset. From [53].

terrace indicating that either the growth is slower there or that they dissolve in supplying material for the larger QDs.

Now we turn to the orientation of the QDs. Fig. 5 depicts some QDs together with the wetting layer in between. The latter consists of protruding stripes running along $[\bar{1}\,1\,0]$ with a $\times 4$ periodicity in $[1\,1\,0]$ direction in agreement with observations of other groups [21,24]. This structure is the same as observed on the InAs(2×4) surface [54]. From the atomic structure of the wetting layer, the azimuthal orientation of the sample can be derived. With this information we are able to determine the relative orientation of the QDs on the substrate. This is clearly seen from the contour plots in Fig. 6(a) where we have indicated the rather straight sections approximately along $[\bar{3}\,1\,0]$, inclined by $24^\circ \pm 2^\circ$ against $[\bar{1}\,1\,0]$, between the QD envelope and the substrate surface. As these intersections are rather straight, one can conclude that the envelope of the QD consists of planar facets. In Fig. 6(c) we have sketched contours for model QDs with different low-index facets as discussed by

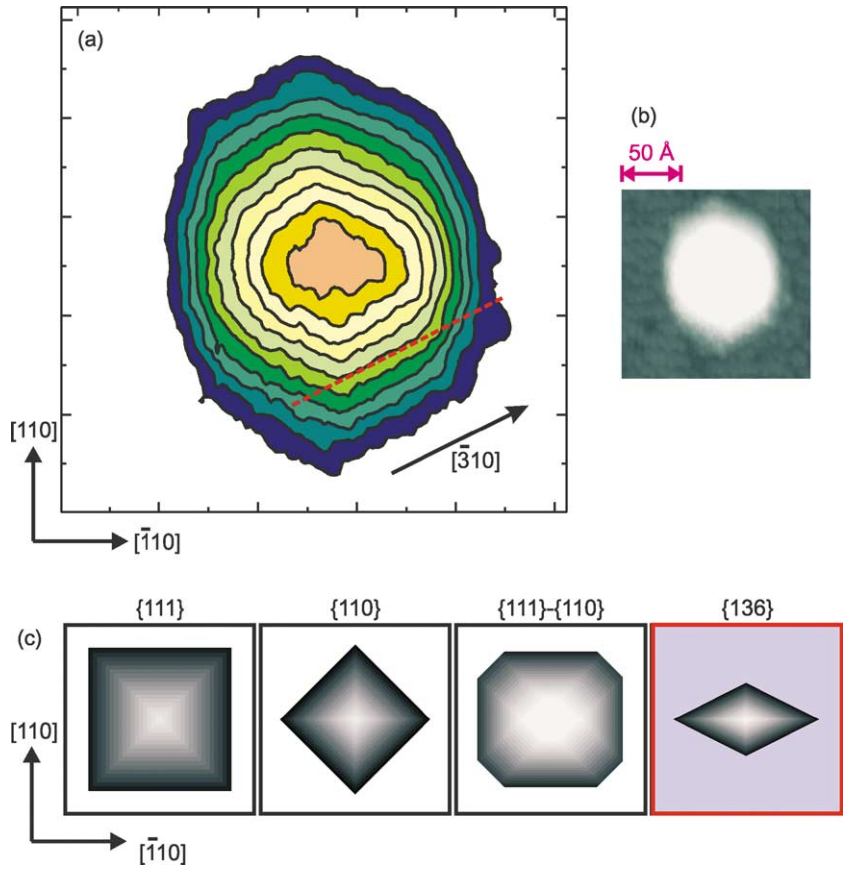

Fig. 6. (a) Contour plot of a InAs QD on GaAs(0 0 1). (b) The same QD with a gray scale appropriate to depict the wetting layer. (c) Contour plots for some model QDs. From [53].

Moll et al. [14] including the contour for a dot with {1 3 6} facets according to the proposal of Lee et al. [20]. It is interesting to note that the intersection of the facet on our QD agrees only with the Lee proposal. This is not in contradiction to our result because {1 3 7} and {1 3 6} have the same line of intersection with the (0 0 1) substrate.

With our method we have been able to atomically resolve the shape of single QDs. One example is shown in Fig. 7. It is turned by computer such that the right facet in the foreground is observed best. The oblong objects were identified as arsenic dimers. The (1 3 7) unit cell is indicated. This surface is different from any low-index III–V surface known till recently. It could be identified only by knowing the GaAs(2 5 11) surface which had been discovered recently in our group [41–43]. Fig. 8 exhibits the model of the GaAs(2 5 11) surface as derived from atomically resolved STM images and ab initio total energy calculations [41–43]. In the (2 5 11) unit cell one recognizes three As dimers which are arranged in a (1 3 7) configuration. The (2 5 11) unit cell consists of scales two (1 3 7) unit cells large. The (1 3 7) facet may be not so far off in energy, although it does not fulfill the electron counting rule [55,56]. Probably it becomes stabilized from the edges of the small facets on the quantum dot. Actually, in the mean time we have observed also (2 5 11)-like facets on these kinds of QDs so that the (1 3 7) facets likely are only metastable.

The knowledge of the unit cell of the facet is crucial in determining its exact orientation. The latter is not possible from the RHEED or LEED data since their absolute accuracy in determining angles is only $\pm 5^\circ$ and the orientations derived from the existent measurements are all within several degrees only: (1 3 6) [20], (1 2 5)

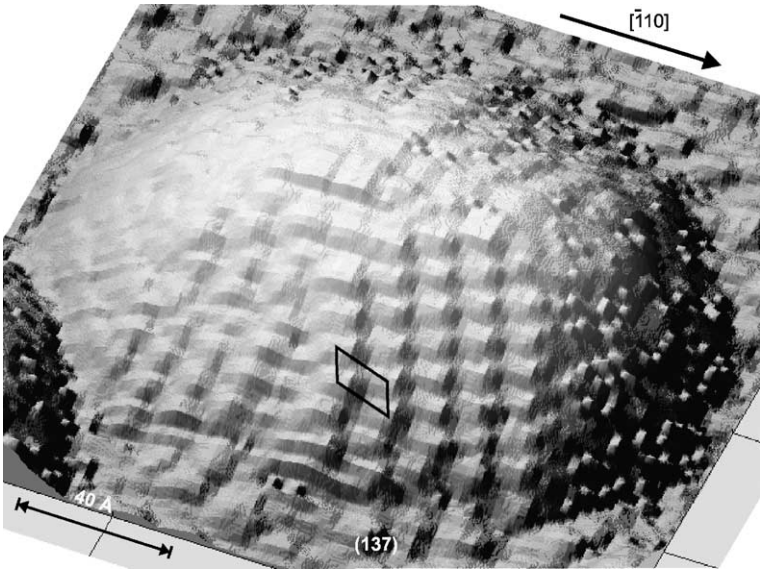

Fig. 7. 3-D STM image of an uncovered InAs QD grown on GaAs(0 0 1). The image is turned such that the right-hand facet in the foreground is seen best. The unit cell of the (1 3 7) facet is indicated. From [43].

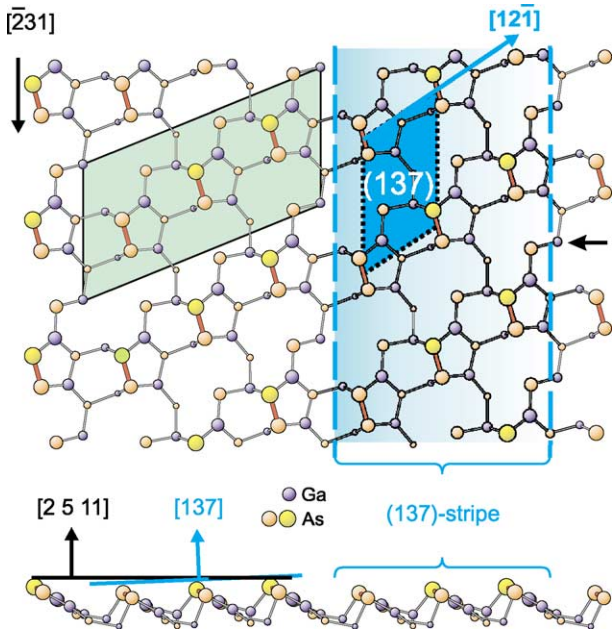

Fig. 8. Model of the GaAs(2 5 11) surface in top and side view. On the left-hand side the (2 5 11) unit cell (light green background) and on the right-hand side the (1 3 7) unit cell (blue background) is given.

[19], or (1 3 7) [22]. However, knowing the unit cell allows a very easy decision. This is well recognized from Fig. 9. The size and symmetry of the unit cells of the mentioned facets differ strongly and the measured data agree only with those for the (1 3 7) facet so that we can exclude (1 3 6) and (1 2 5).

With this information we have been able to derive an atomically resolved model of the InAs QDs on GaAs(0 0 1) which is depicted in Fig. 10 together with a measured STM image. One sees that about 80% of the whole surface is terminated by (1 3 7) facets. The smaller {1 1 0} and {1 1 1} ones were not resolved with the STM. They are included in the model as a reasonable means to geometrically confine the {1 3 7} facets. The model is also in very good agreement with the RHEED results as demonstrated in Fig. 11. Interestingly, the cross section through the QD changes strongly with azimuthal angle although both are cleavage planes. This has to be also taken into account in X-STM. Fig. 11 presents an elucidating correlation between the three-dimensional shape, the cross-sections derived from them, and the RHEED pattern. In the middle-row pictures the electron beam running along [1 1 0] opposes the—from this direction rather steep—{1 3 7} facets. The concomitant reflexes are way out of the RHEED screen. However, when the electrons impinge along [1 $\bar{1}$ 0], they oppose the {1 3 7} facets which now are only slightly tilted against this direction and the additional reflexes can be observed at the RHEED screen giving rise to the chevron-like features.

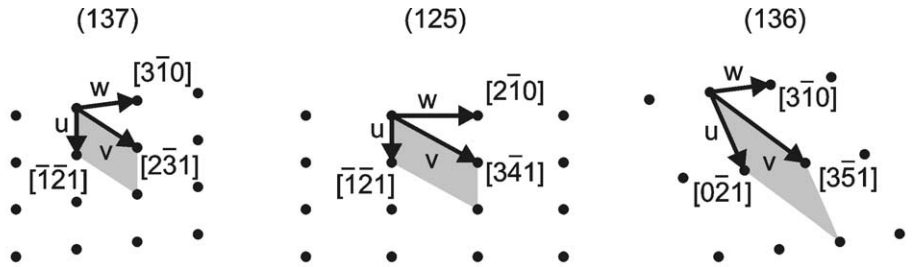

Surface	Experiment	(137)	(125)	(136)
u /Å	6.5 ± 0.1	6.9 +	6.9 +	12.6 —
v /Å	10.5 ± 0.2	10.6 +	14.4 —	17.4 —
w /Å	9.0 ± 0.3	8.9 +	12.6 —	8.9 +
Angle (u ,w) /°	82.4 ± 0.7	82.6 +	90.0 —	73.6 —

Fig. 9. Schematic drawing of the (1 3 6), (1 3 7), and (1 2 5) unit cells. A comparison between the geometrical data from experiment and the models is given in the table below.

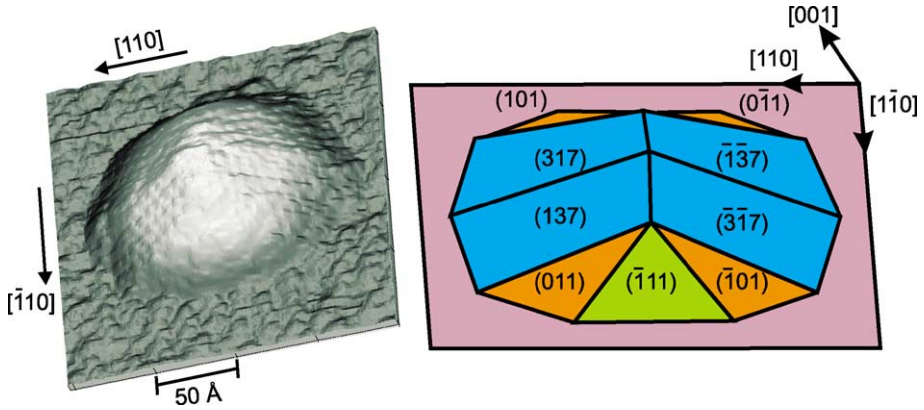

Fig. 10. Left-hand side: STM image of a InAs QD on GaAs(0 0 1). Right-hand side: Model derived from the STM data.

In summarizing we underline that our QDs are well in the range of parameters of preparation used and geometrical sizes observed by other groups. So, we are not presenting results in any special corner of the parameter space. To the main part, the dots are not terminated by low-index surfaces as speculated for many years [14–16,45,46 and others]. The discovery of a stable low-energy surface as (2 5 11) within the stereographic triangle was very surprising. The (1 3 7) facet is a structural element of this surface and may be not so far off in energy, although it does not fulfill the electron counting rule [55,56]. It may well be that the (1 3 7) facet becomes stabilized from the edges on the quantum dot. Furthermore, we note that the QD is rather flat with an angle of only 21° relative to the substrate which is about half of that expected

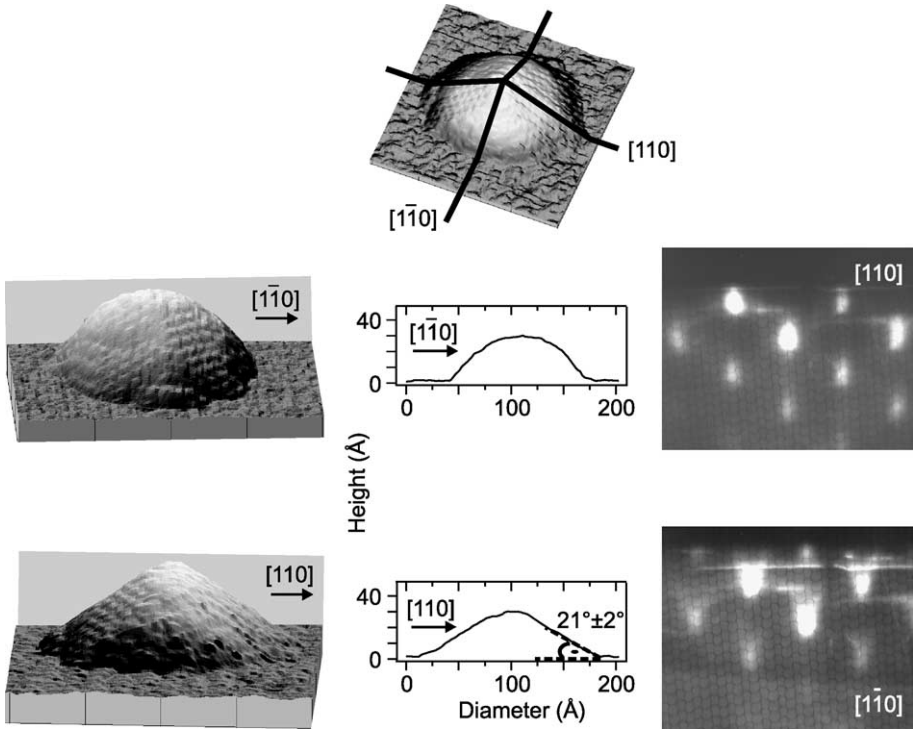

Fig. 11. Height profiles through the center of an InAs QD on GaAs(0 0 1) parallel to [1 $\bar{1}$ 0] in the middle picture row and parallel to [1 1 0] in the bottom picture row. The profile direction is also indicated in the 3-D STM image on top. On the left-hand side the respective 3-D STM images are depicted. On the right-hand side RHEED pattern are depicted with the electron-beam direction indicated. From [22,53].

for a (1 1 0) facet. The flatness of the QD is a quite general result, independent of substrate orientation, as confirmed for the other substrates discussed below.

5. InAs quantum dots on GaAs($\bar{1}\,\bar{1}\,\bar{3}$)B

Rather early attempts have been made to study QD formation on substrates of orientations other than (0 0 1), e.g., on the GaAs($\bar{1}\,\bar{1}\,\bar{3}$)B surface, for which InAs QDs have been investigated using atomic force microscopy [32,57,58] or ex situ STM from decaped samples [29,59]. A more or less rounded shape has been observed always and Miller indices of single bounding facets of the QDs have not been reported yet. Also, to our knowledge there is no report on any in situ STM investigation for ($\bar{1}\,\bar{1}\,\bar{3}$)B substrates until now. Recently, we have reported atomically resolved STM images of InAs QDs measured in situ after MBE growth on the GaAs($\bar{1}\,\bar{1}\,\bar{3}$)B surface [60]. The bare GaAs($\bar{1}\,\bar{1}\,\bar{3}$)B surface is an appropriate substrate as its stability has been demonstrated earlier [38–40].

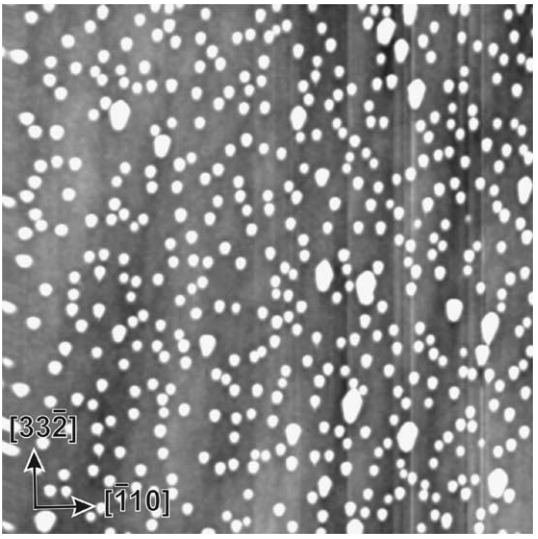

Fig. 12. An overview STM image of InAs QDs grown on the GaAs($\bar{1}\,\bar{1}\,\bar{3}$)B surface (sample bias voltage $U = -3$V; sample current $I = 0.1$ nA). The image size is 1×1 μm^2. The growth temperature was 450 °C and the nominal thickness of deposited InAs was 1.4 (1 1 3)-ML. From [60].

Fig. 12 shows an overview STM image of an ensemble of typical InAs QDs grown on the GaAs($\bar{1}\,\bar{1}\,\bar{3}$)B surface [60]. Two types of 3-D islands are observed: Some large islands and many relatively small islands or QDs of remarkably uniform size. For growth temperatures between 435 and 470 °C the shape of the QDs does not change significantly, whereas the size slightly increases with temperature [61]. The mean diameter at the base and the height of the QDs in Fig. 12 are about 30 and 5nm, respectively giving rise to an aspect ratio of AR = 0.17. In contrast, the large islands do not reveal such a uniform shape and narrow size distribution. Therefore, they are attributed to incoherent 3-D islands, relaxed by incorporating dislocations [62]. They are not further considered here.

Fig. 13 exhibits 3-D STM images of a typical QD viewed along (a) [3 3 $\bar{2}$] and (b) [$\bar{3}\,\bar{3}$ 2]. Since we have atomically resolved the wetting layer, we can determine the azimuthal orientation of the dots. Each QD develops in the same orientation relative to the substrate, with mirror symmetry to the ($\bar{1}$ 1 0) plane normal to the surface. The intersection line between ($\bar{1}$ 1 0) and ($\bar{1}\,\bar{1}\,\bar{3}$)B runs along [3 3 $\bar{2}$]. The ($\bar{1}$ 1 0) plane is also a plane of mirror symmetry on the bulk-truncated ($\bar{1}\,\bar{1}\,\bar{3}$)B surface. So, the symmetry of the bulk-truncated substrate is transferred to the QD proving its epitaxial growth. The main part of the QD is terminated by the facets A and B and a rounded region *E*. Furthermore, one recognizes that the QD comprises a flat base with facets marked by C and D.

Fig. 14 shows high-resolution STM images of the four facets A to D. The facets of type A are {1 1 0} planes as derived from the following facts: The facet A is inclined to the ($\bar{1}\,\bar{1}\,\bar{3}$)B surface by $29 \pm 2°$ and the lengths of the unit-cell vectors on the facet

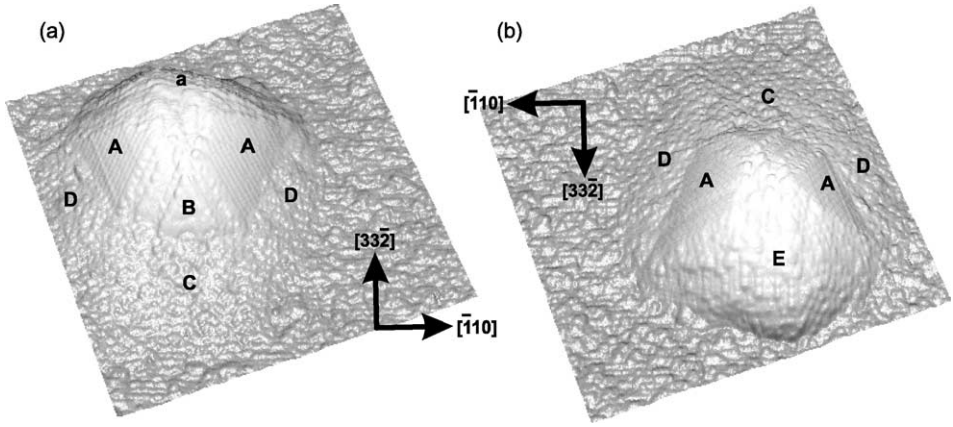

Fig. 13. An InAs QD on GaAs($\bar{1}\,\bar{1}\,\bar{3}$)B depicted from two opposite directions in a 3-D STM image (sample bias voltage $U = -3$ V; sample current $I = 0.1$ nA). The image size is 42×42 nm^2. From [60].

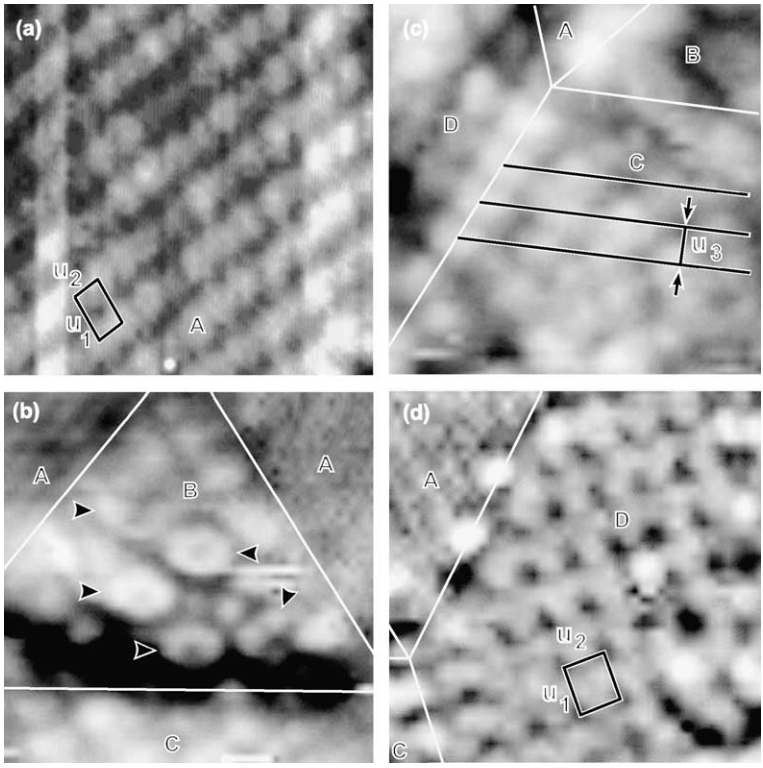

Fig. 14. Atomically resolved STM images of the four facets A, B, C, and D (sample bias voltage $U = -3$ V; sample current $I = 0.1$ nA). The image sizes are (a) 4.3×4.3 nm^2, (b) 9.6×9.6 nm^2, (c) 8.6×8.6 nm^2 and (d) 7.8×7.8 nm^2. From [60].

are $u_1 = 0.56 \pm 0.01$ nm and $u_2 = 0.39 \pm 0.02$ nm; these values agree with the geometric angle of 31.5° between the $(0\,\bar{1}\,\bar{1})$ or $(\bar{1}\,0\,\bar{1})$ and $(\bar{1}\,\bar{1}\,\bar{3})$B planes and with the lengths of the InAs (GaAs) $(0\,\bar{1}\,\bar{1})$ unit-cell vectors projected onto $(\bar{1}\,\bar{1}\,\bar{3})$B which are $u_1 = 0.58$ (0.54) nm and $u_2 = 0.39$ (0.36) nm. The STM image in Fig. 14(a) is also very similar to that acquired on a GaAs(1 1 0) surface [63].

The facet B is $(\bar{1}\,\bar{1}\,\bar{1})$B oriented as concluded from the following facts: It is of triangular shape which is a structural feature of the {1 1 1} surface; also, it is inclined to $(\bar{1}\,\bar{1}\,\bar{3})$B by $28 \pm 1°$ which agrees with the geometric angle of 29.5° between $(\bar{1}\,\bar{1}\,\bar{1})$B and $(\bar{1}\,\bar{1}\,\bar{3})$B. Rings of 0.86 ± 0.08 nm in diameter, indicated by arrowheads in Fig. 14(b), are observed on the facet B, which is considered to be the same kind of structural feature observed on the GaAs$(\bar{1}\,\bar{1}\,\bar{1})$ B$(\sqrt{19} \times \sqrt{19})$ surface [64,65]. Although the rings are not ordered with respect to the $(\sqrt{19} \times \sqrt{19})$ unit cell, this is not necessarily excluding our interpretation, since such a disordered array of rings was reported also on the flat GaAs$(\bar{1}\,\bar{1}\,\bar{1})$B surface (for example see Fig. 3 in Ref. [65]) and well ordered $\sqrt{19} \times \sqrt{19}$ domains may not easily form on a small facet.

The facet C on the base of the QD is considered to be of $(\bar{1}\,\bar{1}\,\bar{2})$B orientation from the following facts: The intersection lines of facet C with $(\bar{1}\,\bar{1}\,\bar{3})$B and also with $(\bar{1}\,\bar{1}\,\bar{1})$B (the facet B) are parallel to $[\bar{1}\,1\,0]$ which indicates that the facet C has Miller index $(\bar{h}\bar{h}\bar{k})$ with $1 < k/h < 3$; also, the facet C is inclined to $(\bar{1}\,\bar{1}\,\bar{3})$B by $11 \pm 2°$ which agrees with the geometric angle of 10.0° between $(\bar{1}\,\bar{1}\,\bar{2})$B and $(\bar{1}\,\bar{1}\,\bar{3})$B. Although it is difficult to recognize the exact unit cell, rows of humps are seen which can be connected by lines of a given separation $u_3 = 0.92 \pm 0.03$ nm in accordance with 1.03(0.96) nm, the geometric length of a $(\bar{1}\,\bar{1}\,\bar{2})$B unit-cell vector perpendicular to $[\bar{1}\,1\,0]$ and projected onto $(\bar{1}\,\bar{1}\,\bar{3})$B. However, it has been reported that the GaAs$(\bar{1}\,\bar{1}\,\bar{2})$B surface on a flat wafer is not stable and is facetted into other low-index surfaces [66–68]. Therefore, the assignment of the $(\bar{1}\,\bar{1}\,\bar{2})$B facet is doubtful.

The facets D are considered to be of $\{\bar{1}\,\bar{3}\,\bar{5}\}$B orientation from the following facts: The facets D are inclined to $(\bar{1}\,\bar{1}\,\bar{3})$B by $13 \pm 1°$, the lengths of the unit-cell vectors are $u_1 = 1.01 \pm 0.04$ nm and $u_2 = 0.94 \pm 0.04$ nm, and the angle between u_1 and u_2 is $89 \pm 2°$. These values agree with the geometric angle of 14.5° between $(\bar{1}\,\bar{3}\,\bar{5})$B and $(\bar{1}\,\bar{1}\,\bar{3})$B, with the unit-cell vectors of $(\bar{1}\,\bar{3}\,\bar{5})$B projected onto $(\bar{1}\,\bar{1}\,\bar{3})$B that are $u_1 = 1.12$ (1.05) nm and $u_2 = 1.07$ (1.00) nm, and with the angle of 92° between the $(\bar{1}\,\bar{3}\,\bar{5})$B unit-cell vectors projected onto $(\bar{1}\,\bar{1}\,\bar{3})$B. Moreover, an angle between $[\bar{1}\,1\,0]$ and an intersection line of the facet D with the facet C is $67 \pm 1°$. This value agrees with the geometric angle of 67.5° between $[\bar{1}\,1\,0]$ and $[13\,35\,\overline{16}]$, the intersection line between $(\bar{1}\,\bar{3}\,\bar{5})$B and $(\bar{1}\,\bar{1}\,\bar{2})$B, projected onto $(\bar{1}\,\bar{1}\,\bar{3})$B. The intersection line is parallel to the unit vector u_1 on the facet D as seen in Fig. 14(c) or (d) also in accordance with a feature of the $(\bar{1}\,\bar{3}\,\bar{5})$B surface. To our knowledge, this is the first indication that $(\bar{1}\,\bar{3}\,\bar{5})$B may be a stable surface by its own. In the mean time it became clear to us that the observed unit cell is due to a c(2×2) rather than a (1×1) unit cell.

From pure geometrical considerations, the center part of the rounded region E in Fig. 13 consists of $(0\,0\,\bar{1})$ which is inclined to $(\bar{1}\,\bar{1}\,\bar{3})$B by 25°. The rounded region E, which is not shown in detail here, does not exhibit an ordered surface structure. Because of its high symmetry, the $(0\,0\,\bar{1})$ surface does not have step structures, strongly asymmetric with respect to the azimuth. The ability to form somehow round

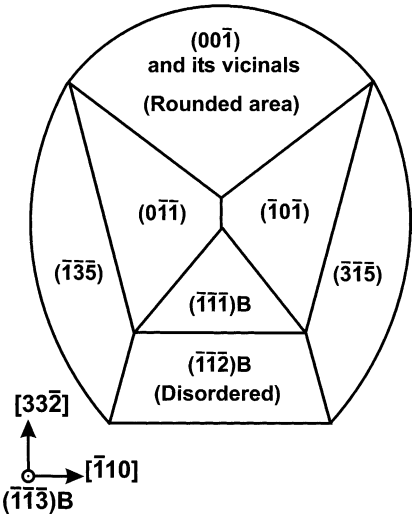

Fig. 15. Schematic drawing of the InAs QD shape on GaAs($\bar{1}\,\bar{1}\,\bar{3}$)B. From [60].

steps makes it plausible that also a round cap at the dot is formed based on (0 0 $\bar{1}$) and its vicinal surfaces.

In summary, the shape of InAs QDs grown on the GaAs($\bar{1}\,\bar{1}\,\bar{3}$)B surface could be derived from atomically resolved STM images. A model is depicted in Fig. 15. Interestingly, the main part of the QD sits on a flat base composed of high-index surfaces such as ($\bar{1}\,\bar{3}\,\bar{5}$)B, ($\bar{3}\,\bar{1}\,\bar{5}$)B, and probably ($\bar{1}\,\bar{1}\,\bar{2}$)B. The shape of the main part of the QD is composed of (0 $\bar{1}$ $\bar{1}$), ($\bar{1}$ 0 $\bar{1}$), and ($\bar{1}\,\bar{1}\,\bar{1}$)B facets and a rounded region that is considered to be composed of (0 0 $\bar{1}$) and its vicinal surfaces. Interestingly, ($\bar{1}\,\bar{1}\,\bar{1}$)B and {1 1 0} low-index surfaces are observed here as the main bounding facets for InAs QDs on the high-index GaAs($\bar{1}\,\bar{1}\,\bar{3}$)B substrate whereas high-index {1 3 7} facets have been found as bounding facets for InAs QDs on the low-index GaAs(0 0 1) surface [22].

6. InAs quantum dots on GaAs(1 1 3)A

The GaAs(1 1 3)A surface turned out to be an appropriate substrate as it is a stable low-energy surface with its own characteristic (8×1) reconstruction. Low defect and dislocation density for InAs/GaAs(1 1 3)A interfaces has been already reported from photoluminescence measurements [30,69,70]. The structural properties of the QDs were investigated using atomic force microscopy [70] or ex situ STM from decapped samples [71]. An arrowhead-like shape has been observed and attributed to "faceting of the GaAs(1 1 3)A surface" without giving any further detail [71]. The Miller indices of the QD bounding facets have not been determined yet and there is no report on any in situ STM investigations for QDs on GaAs(1 1 3)A. We

have studied InAs QDs on GaAs(1 1 3)A with in situ STM observations following MBE growth [72].

Fig. 16 shows an STM image of InAs QDs grown on GaAs(1 1 3)A. The critical thickness at which the QDs are formed at 450 °C is 2.5 ± 0.3 (1 1 3)-ML for the A face compared to 1.7 ± 0.3 (1 1 3)-ML for the B face discussed above. The later onset of the SK growth on the A face may be explained by the partial relaxation of InAs in the long 3-D hills observed already on the wetting layer. A similar delay was found for $In_{0.5}Ga_{0.5}As$ grown on GaAs(3 1 1)A and (1 0 0) [73].

The different size distribution of the islands on GaAs(1 1 3)A (Fig. 16) and on GaAs($\bar{1}\,\bar{1}\,\bar{3}$)B (Fig. 12) is apparent: While the QDs on the B face are very uniform in size, there are many small and large dots on the A face. The measured lengths along [$\bar{3}\,\bar{3}$ 2] are distributed on the (1 1 3)A surface from 300 to 600 Å with the maximum of 35% at 400 Å; on the ($\bar{1}\,\bar{1}\,\bar{3}$)B surface from 200 to 400 Å with a maximum of 45% at 350 Å. The number density is 3×10^{10} cm^{-2} on ($\bar{1}\,\bar{1}\,\bar{3}$)B and 9.5×10^{9} cm^{-2} on (1 1 3)A. Because of the highly disordered undulating morphology [72], the (1 1 3)A surface exhibits a very inhomogeneous strain distribution before the SK growth. There are very likely locations where the strain is better relieved which may be considered as potential nucleation sites for the QDs. Therefore, we conclude that the nucleation and growth process does not start simultaneously on the whole surface. Indeed, many small nuclei, that are not grown up to QDs, can be seen in Fig. 16 whereas they are absent in Fig. 12 for ($\bar{1}\,\bar{1}\,\bar{3}$)B. These observations illustrate a so-called nucleation-limited growth of QDs on GaAs(1 1 3)A and do not confirm the recently reported explanation of the arrow-head like shape due to larger diffusion

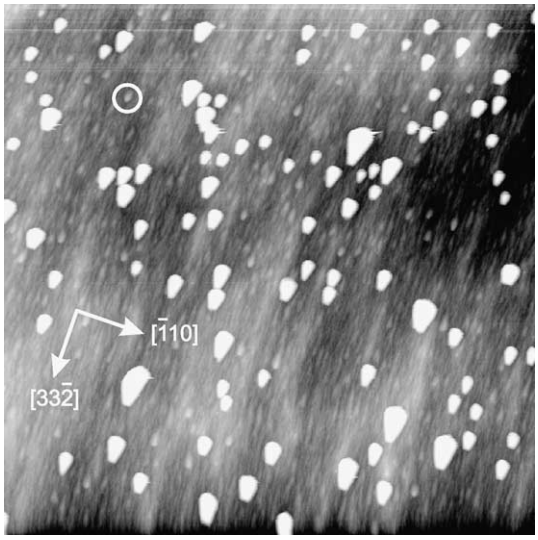

Fig. 16. Overview STM image of InAs QDs grown on GaAs(1 1 3)A (sample bias voltage $U = -3$ V; sample current $I = 0.1$ nA). One presumed nucleus is highlighted by a white circle. The size is 1 μm × 1μm. The growth temperature was 450 °C and the nominal InAs thickness was 2.5 (1 1 3)-ML. From [72].

length of In atoms on GaAs(1 1 3)A with respect to GaAs($\bar{1}\,\bar{1}\,\bar{3}$)B [74]: The larger diffusion length on the A face would narrow the size distribution since smaller islands grow faster than larger ones [75] as opposed to what is observed in the experiment.

The shape of the InAs QDs on GaAs(1 1 3)A obviously differs from that on GaAs($\bar{1}\,\bar{1}\,\bar{3}$)B. This is even better recognized from Fig. 17 which shows an STM

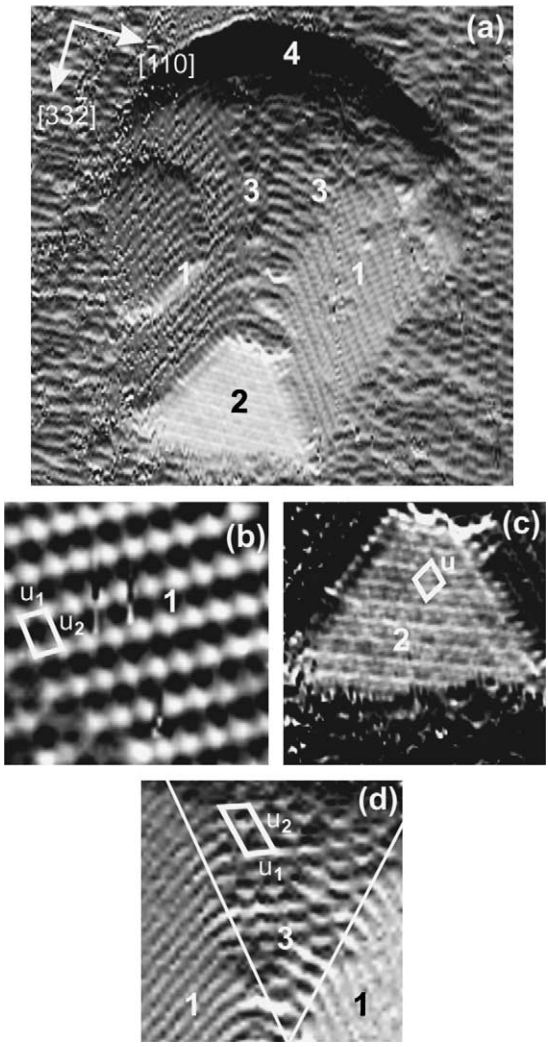

Fig. 17. Atomically resolved STM images (error signal ≡ constant height mode) of (a) a QD on GaAs(1 1 3)A with four characteristic regions (28.3×28.3 nm^2, sample bias voltage $U = -3$ V; sample current $I = 0.322$ nA), (b) the (0 1 1) or (1 0 1) facet (3.7×3.7 nm^2, $U = -3.1$ V, $I = 0.135$ nA), (c) the (1 1 1)A-(2×2) reconstructed facet (9.8×9.8 nm^2, $U = -3$ V, $I = 0.322$ nA), and (d) {2 5 11}A(1×1) reconstructed facets on the summit of the QD (11×11 nm^2, $U = -2.5$ V, $I = 0.33$ nA). From [72].

image of a typical small InAs QD. The exact azimuthal directions on the substrate were determined from the atomically resolved wetting layer as well as from the wafer manufacturer data. The dot exhibits mirror symmetry with respect to the $(\bar{1}\,1\,0)$ plane normal to the surface. The island comprises two symmetrical facets 1, one frontal facet 2, small facets 3 on the summit, and a rounded region 4.

The facets 1 shown in Fig. 17(b) are identified as $\{1\,1\,0\}$ planes from the STM measurements: The facets are inclined to the (1 1 3)A substrate by $29 \pm 4°$ and exhibit the unit-cell vectors of $u_1 = 3.8 \pm 0.2$ Å and $u_2 = 5.5 \pm 0.2$ Å, in good accord with the geometrical angle of 31.5° between (0 1 1) or (1 0 1) planes and (1 1 3)A, and with the lengths of the InAs(GaAs) $\{1\,1\,0\}$ unit-cell vectors projected onto (1 1 3)A, which are equal to $u_1 = 3.9$ (3.6) Å and $u_2 = 5.8$ (5.4) Å. It is interesting to note that on the left facet 1 (on the (1 0 1) surface) a 2-D island with the monatomic step height expands in the middle of the facet from bottom towards the middle giving the impression that the nucleation of a new layer had started at the bottom. This site was calculated to be of the highest strain energy [14,75]. Therefore we suppose that local variations of the misfit strain on the QD does not play a crucial role in the nucleation and growth. From the fact that we observe the 2-D island, we conclude that the $\{1\,1\,0\}$ facets on the islands on GaAs(1 1 3)A grow rather slowly.

The triangular facet 2, shown better resolved in Fig. 17(c) is the (1 1 1)A reconstructed surface as derived from following measurements: It is inclined to (1 1 3)A by $26° \pm 4°$ and exhibits the diamond-shaped unit cell with the vector $u = 8.0 \pm 0.4$ Å; these values agree with the geometrical angle of 29.5° between (1 1 1)A and (1 1 3)A planes and with the length of the projected onto (1 1 3)A InAs(GaAs) unit-cell vector of In(Ga) vacancy buckling model [76] for the (1 1 1)A-(2×2) reconstruction, $u = 7.8$ (7.2) Å. The filled state STM image in Fig. 16(c) is very similar to that acquired from the planar GaAs(1 1 1)A-(2×2) surface [77].

The small facets 3 on the summit of the island are $\{2\,5\,11\}$A reconstructed surfaces as extracted from the following measurements: The angle to the substrate and the lengths of the unit-cell vectors are $7 \pm 3°$, $u_1 = 11.5 \pm 0.5$ Å and $u_2 = 21.7 \pm 1.0$ Å, respectively. These values are in agreement with the geometrical angle of 10.0° between (2 5 11)A or (5 2 11)A and (1 1 3)A, and with the lengths of the InAs(GaAs) unit-cell vectors for the $\{2\,5\,11\}$A-(1×1) reconstruction, projected onto (1 1 3)A [41,42], $u_1 = 11.3$ 10.5) Å and $u_2 = 20.2$ (18.8) Å. The small $\{2\,5\,11\}$A facets are considered to be residual elements that vanish from the QDs when they reach their final form. Probably, the QDs start to grow from the wetting layer with the flattest stable, low-energy surface. Due to the tilted geometry [41,42], the $\{2\,5\,11\}$ surface grows relatively fast and disappears after a while leaving behind the slowly growing and energetically more favorable $\{1\,1\,0\}$ facets.

The region 4 in Fig. 17(a) exhibits a complex structure that appears rounded on the small QDs. From geometrical considerations, a (0 0 1) surface—inclined to (1 1 3) by 25°—should develop in this area. From experiments of simultaneous growth of low-index surfaces on patterned GaAs substrates it is known that (0 0 1) facets grow with the largest rate [78–80]. The main reason may be found in the fact that on this surface As_2 molecules can be incorporated without dissociation [81,82]. Therefore, we believe that also the rounded region grows with the highest rate which is certainly

further increased by a presumed high step and kink density which altogether prevents us from acquiring atomically resolved images from this region.

After some growth, the shape of the QDs change appreciably and the QDs adopt the arrowhead-like shape recognized already from Fig. 16. As seen from Fig. 18(a), the {1 1 0} facets are much longer in [3 3 $\bar{2}$] direction and the (1 1 1)A facet exhibits a drastic reduction in size in comparison to the QD in Fig. 17(a). Also, two flat surfaces form in the vicinal (0 0 1) region that were identified as ($\bar{1}$ 1 3)B and (1 $\bar{1}$ 3)B. They are perfectly connected with the {1 1 0} facets as shown in Fig. 18(b). The ($\bar{1}$ 1 3)B and (1 $\bar{1}$ 3)B surfaces are inclined to (1 1 3) by $40 \pm 5°$ and exhibit unit-cell vectors of $u_1 = 4.1 \pm 0.2$ Å and $u_2 = 13.0 \pm 0.3$ Å (geometry values for the bulk truncated ($\bar{1}$ $\bar{1}$ $\bar{3}$)B surface: 35.1°, 3.9 Å, 13.7 Å). The {2 5 11}A facets expected at the summit are largely reduced in size.

The elongation of the QDs was reported to give rise to a polarization anisotropy [71] that may become effective in polarization-sensitive devices. So, one may ask why the QDs become elongated along [3 3 $\bar{2}$]. Such a behavior means that at one moment during growth mainly (1 1 1)A continues to grow whereas the growth in the rounded region and at the {1 1 0} facets is slowed down. Thus—owing to geometrical reasons—(1 1 1)A becomes smaller so that extended {1 1 0} surfaces form on both sides of the QD and the QD acquires a modified shape.

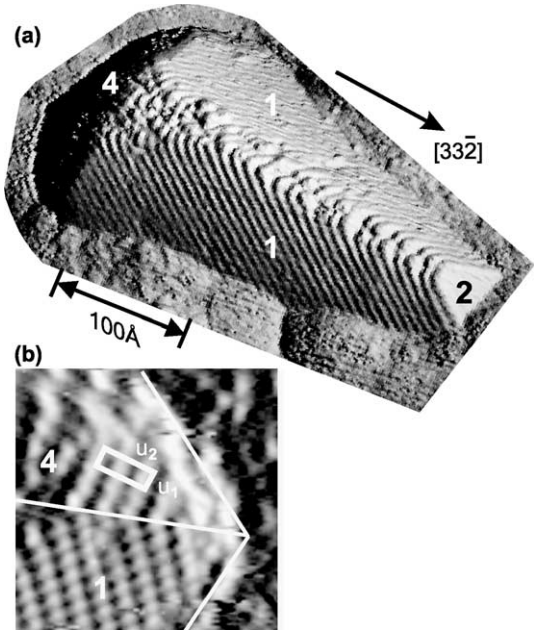

Fig. 18. (a) 3-D STM image of an elongated InAs QD grown on GaAs(1 1 3)A (sample bias voltage $U = -2.5$ V; sample current, $I = 0.33$ nA), (b) the border between the (0 1 1) and the ($\bar{1}$ 1 3)B(1×1) facet (6.3×6.3 nm^2, $U = -3.1$ V, $I = 0.135$ nA). From [72].

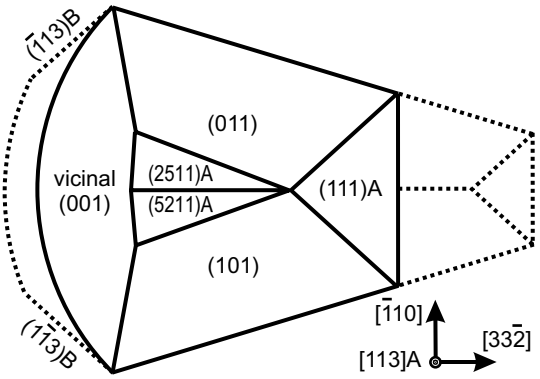

Fig. 19. Schematic sketch of shape and bounding facets of an InAs QD on GaAs(1 1 3)A. The solid line represents the QD shape briefly after the appearance of QDs; the dotted line represents elongated QDs after further growth. From [72].

The slowing down in relative growth rate at the rounded region is obviously inferred from the evolution of the GaAs$\{\bar{1}\,\bar{1}\,\bar{3}\}$B facets. For $\{\bar{1}\,\bar{1}\,\bar{3}\}$B, the growth rate is probably lower than for {0 0 1} as the As_2 molecules have to be dissociated prior to incorporation [81,82]. Also, the {1 1 0} and $\{\bar{1}\,\bar{1}\,\bar{3}\}$B facets seem to fit very smoothly at the edge in between (see Fig. 18(b)) which furthermore decreases the growth rate in this region and also on the {1 1 0} facet because the perfect edge does not supply favorable adsorption sites. Once started to grow, the (1 1 1)A facet decreases in size for geometrical reasons. This reduces the strain and thereby the energy barrier for incorporation of further atoms and thus speeds up the growth rate of the (1 1 1)A facet [75].

Our results for the InAs/GaAs(1 1 3)A system are summarized in Fig. 19. Depending on growth stage, we observe two QD shapes which differ in relative facet sizes but not in symmetry and azimuthal orientation. In the early stage of the growth, the shape of the InAs QDs is given by {1 1 0} and (1 1 1)A bounding facets, {2 5 11}A facets at the summit and a rounded region, probably due to a stacking of vicinal (0 0 1) surfaces (see solid line). Later in the growth, the QDs become elongated along $[3\,3\,\bar{2}]$ with a size reduction of the (1 1 1)A facet induced by a partially flattening of the rounded region (see dotted line) by $\{\bar{1}\,\bar{1}\,\bar{3}\}$B facets which obviously slow down the growth rate in this region. The somewhat broad size distribution indicates growth limitation which may be inferred from the mesoscopically rough (1 1 3)A surface.

7. Comparison between the GaAs(1 1 3)A and GaAs($\bar{1}\,\bar{1}\,\bar{3}$)B substrates

Here, we compare the InAs QDs grown on the two GaAs(1 1 3)A and GaAs($\bar{1}\,\bar{1}\,\bar{3}$)B substrates which exhibit the same orientation but different surface reconstructions. From the orientation of the substrate, the symmetry of the islands

as well as the kind and orientation of the bounding facets derive and are found to be equal on both GaAs{1 1 3} surfaces. This proves that the InAs QDs are grown epitaxially. However, shape, size, and size distribution of the QDs are different: Inhomogeneously distributed, elongated InAs islands on the A face differ from the more uniform, rather round InAs islands on the B face. This difference is not completely understood yet, but one may try to explain it in terms of obvious differences in the mesoscopic structure of the wetting layer. The latter may influence the inter-surface diffusion of In atoms from slower to faster growing facets and thus may influence size, size distribution, and shape of the QDs. This problem waits for modeling with the next-generation computer power. Although this topic will be more thoroughly discussed in a future contribution [83], we will briefly present some arguments in the following.

At 450 °C, the bare GaAs(1 1 3)A surface exhibits the known (8×1) reconstruction as observed in RHEED and LEED, consisting of zigzag chains of As dimers [36,37]. The chains are directed along $[3\,3\,\bar{2}]$ in two different layers. In addition, the surface exhibits relatively small terraces due to a mesoscopic-scale undulation [43,84–86] which consists of arrowhead-like pits with GaAs(3 7 15)A and (2 5 11)A surfaces on the side walls, surrounded by the (8×1) reconstruction [43]. This mesoscopic structure is not understood yet. The explanation is likely to be kinetic rather than thermodynamic as under As-rich preparation conditions the surface energies of GaAs(3 7 15)A or (2 5 11)A are 53 and 55 meV/Å^2 [41,42], respectively, i.e., higher than the 47 meV/Å^2 for GaAs(1 1 3)A [37]. Depositing InAs, the corrugation of the surface becomes much more pronounced [83]. Any flat region on the surface disappears. Instead of the original (8×1) reconstruction, poorly ordered, long, and arrowhead-like hills are formed pointing along $[\bar{3}\,\bar{3}\,2]$ and exhibiting walls built up from (3 7 15)A, (2 5 11)A and (1 3 7)A facets. With the increase of the InAs coverage, the height and periodicity of these hills increase from 0.6 ± 0.3 and 5.0 ± 3.0 nm at the beginning to 1.3 ± 0.3 and 30.0 ± 20.0 nm, respectively, at the onset of appearance of high 3-D QDs. The same wetting layer behavior was observed by depositing $In_{0.5}Ga_{0.5}$ As onto GaAs(1 1 3)A [73]. The reason for the strong undulation of the wetting layer is probably the partial relaxation of InAs in the long 3-D hills as well as the drop of the surface free energy of InAs(3 7 15)A, (2 5 11)A and (1 3 7)A to 42, 41 and 44 meV/Å^2, respectively [87]. However, no long-range areas of these facets were observed.

The atomic arrangement on the A and B faces of the GaAs{1 1 3} surface cannot be the same since [1 1 3] is a polar direction. Nevertheless they exhibit rather similar reconstructions. The high-temperature, well-ordered (8×1) reconstruction of GaAs $(\bar{1}\,\bar{1}\,\bar{3})$B exhibits again zigzag chains but now of Ga dimers in the topmost layer [38–40]. So far, this has been concluded from atomically resolved STM images but has not yet been confirmed through a structure determination.On a mesoscopic scale the morphology of the GaAs$(\bar{1}\,\bar{1}\,\bar{3})B(8 \times 1)$ surface differs from that of the A face. The large terraces on the B face do not show any tendency to form any other reconstruction being probably related to the lower surface energy with respect to $(\bar{3}\,\bar{7}\,\overline{15})$B, $(\bar{2}\,\bar{5}\,\overline{11})$B and $(\bar{1}\,\bar{3}\,\bar{7})$B under As-rich preparation condition. At 470–490 °C the surface undergoes a transition to a less well-ordered, more As-rich structure by

adsorbing As atoms and rearranging the Ga dimers into a more flat reconstruction [39]. At 450 °C it exhibits locally a mixed $(2\times1)+(1\times1)$ structure (with respect to the face-centered unit cell), consisting of locally ordered As adatoms and dimers on top of the bulk-truncated $(\bar{1}\,\bar{1}\,\bar{3})$B plane but no long-range order does exist; nevertheless the surface exhibits large terraces separated by well developed steps [39].

With the transition to an As-rich phase, the GaAs$(\bar{1}\,\bar{1}\,\bar{3})$B surface does not change its mesoscopic morphology establishing it as a very flat substrate for InAs heteroepitaxy. This flatness remains during InAs deposition. STM images of the wetting layer (not shown here) exhibit large terraces separated by monatomic steps. Moreover just before the 3-D growth mode sets in, the morphology of the wetting layer is very similar to that on (0 0 1): Small and large 2-D and small 3-D clusters are observed that were considered to be precursors for the growth of the QDs on GaAs(0 0 1) [26]. This indicates that the mechanism of QD formation on GaAs$(\bar{1}\,\bar{1}\,\bar{3})$B is quite similar to that on GaAs(0 0 1) resulting in even better optical properties [32,88]. The above-described different atomic structures of the bare GaAs(1 1 3)A and $(\bar{1}\,\bar{1}\,\bar{3})$B surfaces and of the wetting layers very likely result in different shapes of the InAs QDs.

8. Conclusions

From the numerous studies of InAs QD formation on GaAs(0 0 1) a quite consistent picture emerged: For an InAs thickness between 1.6 ± 0.2 and about 3.0 ML self-assembled QDs are observed. The size is about 25 ± 5 nm in diameter at the base and 5 ± 1 nm in height giving rise to an aspect ratio of $AR=0.20\pm0.05$. There is a tendency to become larger with coverage and with substrate temperature during growth. The number density can vary between 1×10^{10} and 3×10^{11} QDs cm^{-2}. The same orders of magnitude are found for the (1 1 3)A and $(\bar{1}\,\bar{1}\,\bar{3})$B surfaces. In the studies, which are performed with sufficient spatial resolution, an asymmetry in diameter is observed with an elongation along $[1\,\bar{1}\,0]$. This asymmetry is also mirrored in RHEED where chevron-like satellites are observed with the electron beam along $[1\,\bar{1}\,0]$. All these observations are explainable by the shape which evolved from our atomically resolved STM images showing that more than 80% of the surface of an InAs QD on GaAs(0 0 1) are given by four {1 3 7} high-index surfaces.

From the atomically resolved STM images we can determine the shape of the QDs. The quantum ''dots'' are generally rather flat entities better characterized as ''lenses''. The angle between the substrate and the bounding facets is of the order of 20°. This value differs strongly from that one generally anticipated when one is assuming the bounding facets to consist of low-energy low-index surfaces only. This understanding has been revolutionized by the discovery of GaAs(2 5 11) as a low-energy *high-index* surface recently [41–43]. Generally the shape of InAs QDs is dominated by low-index facets on high-index substrates, e.g., here on (1 1 3)A [72] or on $(\bar{1}\,\bar{1}\,\bar{3})$B [61], and vice versa [22]. Also, the symmetry of the QDs derives directly from the ideal unreconstructed substrate surface which unambiguously proves epitaxial growth.

We have compared the InAs QDs on the two GaAs(1 1 3)A and GaAs($\bar{1}\,\bar{1}\,\bar{3}$)B substrates which exhibit the same orientation but different surface reconstructions. From the orientation of the substrate, symmetry of the islands as well as kind and orientation of the bounding facets are derived and found to be equal on both GaAs{1 1 3} surfaces. However, shape, size, and size distribution of the QDs are different: Inhomogeneously distributed, elongated InAs islands on the A face differ from the more uniform, rather round InAs islands on the B face. This difference may be explained in terms of the different mesoscopic structure of the wetting layer. The latter may influence the inter-surface diffusion of In atoms from slower to faster growing facets. This problem waits for modeling with the next generation computer power.

Acknowledgements

We thank G.Ertl for support and P.Geng as well as M. Richard for technical assistance. We are grateful to J. Márquez, T. Suzuki, Y. Temko, and P. Kratzer for discussion. The work was supported by the Deutsche Forschungsgemeinschaft (SFB296, ProjectA2).

References

[1] D. Bimberg, M. Grundmann, N.N. Ledentsov, Quantum Dot Heterostructures, Wiley, Chichester, New York, 1999.
[2] M. Grundmann, Physica E (Amsterdam) 5 (2000) 167.
[3] Y. Masumoto, T. Takagahara (Eds.), Semiconductor Quantum Dots, Springer, Berlin, Heidelberg, 2002.
[4] S. Guha, A. Madhukar, K.C. Rajkumar, Appl. Phys. Lett. 57 (1990) 2110–2112.
[5] I.N. Stranski, L. Krastanow, Sitzungsber. Akad. Wiss. Wien, Math.-Naturwiss. Klasse 146 (1937) 797.
[6] C. Priester, M. Lannoo, Phys. Rev. Lett. 75 (1995) 93–96.
[7] Y. Chen, J. Washburn, Phys. Rev. Lett. 77 (1996) 4046–4049.
[8] C. Ratsch, A. Zangwill, Surf. Sci. 293 (1993) 123–131.
[9] E. Kortucheva, A.M. Turiel, I. Markov, Phys. Rev. B 61 (2000) 16890–16901.
[10] H.T. Dobbs, D.D. Vvedensky, A. Zangwill, J. Johansson, N. Carlson, W. Seifert, Phys. Rev. Lett. 79 (1997) 897–900.
[11] H.M. Koduvely, A. Zangwill, Phys. Rev. B 60 (1999) R2204–R2207.
[12] Ch. Heyn, C. Dumat, J. Cryst. Growth 227–228 (1997) 990–994.
[13] A.-L. Barabási, Appl. Phys. Lett. 70 (1997) 2565–2567.
[14] N. Moll, M. Scheffler, E. Pehlke, Phys. Rev. B 58 (1998) 4566–4571.
[15] L.G. Wang, P. Kratzer, M. Scheffler, N. Moll, Phys. Rev. Lett. 82 (1999) 4042–4045.
[16] L.G. Wang, P. Kratzer, M. Scheffler, N. Moll, Phys. Rev. B 62 (2000) 1897–1904.
[17] Y. Nabetani, T. Ishikawa, S. Noda, A. Sasaki, J. Appl. Phys. 76 (1994) 347–351.
[18] J.M. Moison, F. Houzay, F. Barthe, L. Leprince, E. Andráe, O. Vatel, Appl. Phys. Lett. 64 (1994) 196–198.
[19] Y. Hasegawa, H. Kiyama, Q.K. Xue, T. Sakurai, Appl. Phys. Lett. 72 (1998) 2265–2267.
[20] H. Lee, R. Lowe-Webb, W. Yang, P.C. Sercel, Appl. Phys. Lett. 72 (1998) 812–814.
[21] B.A. Joyce, T.S. Jones, J.G. Belk, J. Vac. Sci. Technol. B 16 (1998) 2373–2380.

[22] J. Márquez, L. Geelhaar, K. Jacobi, Appl. Phys. Lett. 78 (2001) 2309–2311.
[23] D. Leonard, K. Pond, P.M. Petroff, Phys. Rev. B 50 (1994) 11687–11692.
[24] N. Ikoma, S. Ohkouchi, Jpn. J. Appl. Phys. 34 (Part 2) (1995) L724–L726.
[25] G.S. Solomon, J.A. Trezza, A.F. Marshall, J.S. Harris Jr., Phys. Rev. Lett. 76 (1996) 952–955.
[26] R. Heitz, T.R. Ramachandran, A. Kalburge, Q. Xie, I. Mukhametzhanov, P. Chen, A. Madhukar, Phys. Rev. Lett. 78 (1997) 4071–4074.
[27] H. Lee, R.R. Lowe-Webb, W. Yang, P. Sercel, Appl. Phys. Lett. 71 (1997) 2325–2327.
[28] H. Saito, K. Nishi, S. Sugou, Appl. Phys. Lett. 74 (1999) 1224–1226.
[29] M. Henini, S. Sanguinetti, L. Brusaferri, E. Grilli, M. Guzzi, M.D. Upward, P. Moriarty, P.H. Beton, Microelectr. J. 28 (1997) 933–938.
[30] K. Nishi, R. Mirin, D. Leonard, G. Medeiros-Ribeiro, P.M. Petroff, A.C. Gossard, J. Appl. Phys. 80 (1996) 3466–3470.
[31] S. Sanguinetti, S.C. Fortina, A. Miotto, E. Grilli, M. Guzzi, M. Henini, A. Polimeni, L. Eaves, Thin Solid Films 336 (1998) 9–12.
[32] S.C. Fortina, S. Sanguinetti, E. Grilli, M. Guzzi, M. Henini, A. Polimeri, L. Eaves, J. Cryst. Growth 187 (1998) 126–132.
[33] J.G. Belk, J.L. Sudijono, X.M. Zhang, J.M. Neave, T.S. Jones, B.A. Joyce, Phys. Rev. Lett. 78 (1997) 475–478.
[34] H. Yamaguchi, M.R. Fahy, B.A. Joyce, Appl. Phys. Lett. 69 (1996) 776–778.
[35] S.E. Hooper, D.I. Westwood, D.A. Woolf, S.S. Heghoyan, R.H. Williams, Semicond. Sci. Technol. 8 (1993) 1069–1074.
[36] M. Wassermeier, J. Sudijono, M.D. Johnson, K.T. Leung, B.G. Orr, L. Däweritz, K. Ploog, Phys. Rev. B 51 (1995) 14721–14724.
[37] J. Platen, A. Kley, C. Setzer, K. Jacobi, P. Ruggerone, M. Scheffler, J. Appl. Phys. 85 (1999) 3597–3601.
[38] J. Márquez, L. Geelhaar, K. Jacobi, Phys. Rev. B 62 (2000) 9969–9972.
[39] J. Márquez, L. Geelhaar, K. Jacobi, Phys. Rev. B 65 (2002) 165320 (9 pages).
[40] T. Suzuki, Y. Temko, K. Jacobi, Surf. Sci. 511 (2002) 13–22.
[41] L. Geelhaar, J. Márquez, P. Kratzer, K. Jacobi, Phys. Rev. Lett. 86 (2001) 3815–3818.
[42] L. Geelhaar, Y. Temko, J. Márquez, P. Kratzer, K. Jacobi, Phys. Rev. B 65 (2002) 155308 (13 pages).
[43] K. Jacobi, L. Geelhaar, J. Márquez, Appl. Phys. A 75 (2002) 113–127.
[44] M. Meixner, E. Schöll, V.A. Shchukin, D. Bimberg, Phys. Rev. Lett. 87 (2002) 236101 (4 pages).
[45] S. Ruvimov, P. Werner, K. Scheerschmidt, U. Gösele, J. Heydenreich, U. Richter, N.N. Ledentsov, M. Grundmann, D. Bimberg, V.M. Ustinov, A.Yu. Egorov, P.S. Kop'ev, Zh.I. Alferov, Phys. Rev. B 51 (1995) 14766–14769.
[46] O.A. Kosogov, P. Werner, U. Gösele, N.N. Ledentsov, D. Bimberg, V.M. Ustinov, A.Yu. Egorov, A.E. Zhukov, P.S. Kop'ev, Zh.I. Alferov, Appl. Phys. Lett. 69 (1996) 3072–3074.
[47] X.Z. Liao, J. Zou, X.F. Duan, D.J.H. Cockayne, R. Leon, C. Lobo, Phys. Rev. B 58 (1998) R4235–R4237.
[48] W. Wu, J.R. Tucker, G.S. Solomon, S. Harris Jr., Appl. Phys. Lett. 71 (1997) 1083.
[49] B. Legrand, B. Grandidier, J.P. Nys, D. Stiévenard, J.M. Gérard, V. Thierry-Mieg, Appl. Phys. Lett. 73 (1998) 96–98.
[50] H. Eisele, O. Flebbe, T. Kalka, C. Preinesberger, F. Heinrichsdorff, A. Krost, D. Bimberg, M. Dähne-Prietsch, Appl. Phys. Lett. 75 (1999) 106–108.
[51] P. Geng, J. Márquez, L. Geelhaar, J. Platen, C. Setzer, K. Jacobi, Rev. Sci. Instr. 71 (2000) 504–508.
[52] F.M. Ross, J. Tersoff, R.M. Tromp, Phys. Rev. Lett. 80 (1998) 984–987.
[53] J. Márquez, Ph.D. Thesis, Technical University of Berlin, 2001.
[54] S. Ohkouchi, N. Ikoma, I. Tanaka, J. Vac. Sci. Technol. B 12 (1994) 2033–2036.
[55] W.A. Harrison, J. Vac. Sci. Technol. 16 (1979) 1492–1496.
[56] M.D. Pashley, Phys. Rev. B 40 (1989) 10481–10487.
[57] S.P. Guo, A. Shen, Y. Ohno, H. Ohno, Physica E (Amsterdam) 2 (1998) 672–677.
[58] S.P. Guo, A. Shen, F. Matsukura, Y. Ohno, H. Ohno, J. Cryst. Growth 201/202 (1999) 684–688.
[59] S. Sanguinetti, A. Miotto, S. Castiglioni, E. Grilli, M. Guzzi, M. Henini, A. Polimeni, A. Patane, L. Eaves, P.C. Main, Microelectr. J. 30 (1999) 419–425.

[60] T. Suzuki, Y. Temko, K. Jacobi, Appl. Phys. Lett. 80 (2002) 4744–4746.
[61] T. Suzuki, Y. Temko, K. Jacobi, Phys. Rev. B 67 (2003) 045315 (7 pages).
[62] D. Leonard, M. Krishnamurty, C.M. Reaves, S.P. Denbaars, P.M. Petroff, Appl. Phys. Lett. 63 (1993) 3203–3205.
[63] R.M. Feenstra, J.A. Stroscio, J. Tersoff, A.P. Fein, Phys. Rev. Lett. 58 (1987) 1192–1195.
[64] D.K. Biegelsen, R.D. Bringans, J.E. Northrup, L.-E. Swartz, Phys. Rev. Lett. 65 (1990) 452–455.
[65] J.M.C. Thornton, D.A. Woolf, P. Weightman, Appl. Surf. Sci. 123/124 (1998) 115–119.
[66] J. Platen, C. Setzer, P. Geng, W. Ranke, K. Jacobi, Microelectr. J. 28 (1997) 969.
[67] L. Geelhaar, J. Márquez, K. Jacobi, A. Kley, P. Ruggerone, M. Scheffler, Microelectr. J. 30 (1999) 393–396.
[68] K. Jacobi, J. Platen, C. Setzer, J. Márquez, L. Geelhaar, C. Meyne, W. Richter, A. Kley, P. Ruggerone, M. Scheffler, Surf. Sci. 439 (1999) 59–72.
[69] H. Xu, Q. Gong, B. Xu, W. Jiang, J. Wang, W. Zhou, Z. Wang, J. Cryst. Growth 200 (1999) 70–76.
[70] S. Sanguinetti, S.C. Fortina, A. Miotto, E. Grilli, M. Guzzi, M. Henini, A. Polimeni, L. Eaves, Thin Solid Films 336 (1998) 9–12.
[71] M. Henini, S. Sanguinetti, S.C. Fortina, E. Grilli, M. Guzzi, G. Panzarini, L.C. Andreani, M.D. Upward, P. Moriarty, P.H. Beton, L. Eaves, Phys. Rev. B 57 (1998) R6815–R6818.
[72] Y. Temko, T. Suzuki, K. Jacobi, Appl. Phys. Lett.
[73] P.O. Vaccaro, M. Hirai, K. Fujita, T. Watanabe, J. Phys. D: Appl. Phys. 29 (1996) 2221–2228.
[74] C. Lobo, R. Leon, J. Appl. Phys. 83 (1998) 4168–4172.
[75] D.E. Jesson, G. Chen, K.M. Chen, S.J. Pennycook, Phys. Rev. Lett. 80 (1998) 5156–5159.
[76] S.Y. Tong, G. Xu, W.N. Mei, Phys. Rev. Lett. 52 (1984) 1693.
[77] Fig. 1b in A. Ohtake, J. Nakamura, T. Komura, T. Hanada, T. Yao, H. Kuramochi, M. Ozeki, Phys. Rev. B 64 (2001) 045318 (8 pages).
[78] A. Yamashiki, T. Nishinaga, J. Cryst. Growth 198/199 (1999) 1125–1129.
[79] X.Q. Shen, T. Nishinaga, J. Cryst. Growth 146 (1995) 374–378.
[80] S. Hirose, A. Yoshida, M. Yamaura, H. Munekata, Appl. Phys. Lett. 74 (1999) 964–966.
[81] C.G. Morgan, P. Kratzer, M. Scheffler, Phys. Rev. Lett. 82 (1999) 4886–4889.
[82] P. Kratzer, M. Scheffler, Phys. Rev. Lett. 88 (2002) 036102 (4 pages).
[83] Y. Temko, T. Suzuki, P. Kratzer, K. Jacobi, to be published.
[84] M. Pristovsek, H. Menhal, T. Wehnert, J.-T. Zettler, T. Schmidtling, N. Esser, W. Richter, C. Setzer, J. Platen, K. Jacobi, J. Cryst. Growth 195 (1998) 1–5.
[85] R. Nötzel, J. Temmyo, T. Tamamura, Appl. Phys. Lett. 64 (1994) 3557–3559.
[86] L. Geelhaar, J. Márquez, K. Jacobi, Phys. Rev. B 60 (1999) 15890–15895.
[87] P. Kratzer, private communication.
[88] A. Polimeni, M. Henini, A. Patanè, L. Eaves, P.C. Main, G. Hill, Appl. Phys. Lett. 73 (1998) 1415–1417.